ChemComm

Chemical Communications

www.rsc.org/chemcomm

Volume 49 | Number 29 | 14 April 2013 | Pages 2945–3060

ISSN 1359-7345

RSC Publishing

COMMUNICATION

Simon R. Hall *et al.*

Designed 3D architectures of high-temperature superconductors

1359-7345(2013)49:29;1-1

ChemComm

RSC Publishing

COMMUNICATION

View Article Online
View Journal | View Issue

Designed 3D architectures of high-temperature superconductors†

Cite this: *Chem. Commun.*, 2013, **49**, 2974

Received 16th November 2012, Accepted 31st January 2013

DOI: 10.1039/c3cc38271k

www.rsc.org/chemcomm

David C. Green,[a] Martin R. Lees[b] and Simon R. Hall*[a]

Self-supporting superconducting replicas of pasta shapes are reported, yielding products of differing 3D architectures. Functioning high-temperature superconductor wires are developed and refined from replicas of spaghetti, demonstrating a unique sol–gel processing technique for the design and synthesis of novel macroscopic morphologies of complex functional materials.

Sol–gel techniques, where homogeny of reagents is ensured through dissolution in a solvent system, can be employed to yield high quality polycrystalline superconductors in short times and at low cost, enabling the engineering of superconducting architectures. 2D structures, such as films,[1] can be generated through dip coating;[2] Pechini drop-coating, citrate or nitrate methods;[3] or inkjet printing,[4] however there remains necessity for high cost substrates, such as strontium titanate or yttrium barium copper oxide orientated crystals. 1D wires can also be produced through template direction,[5] however this requires the use of expensive, anodised alumina membranes, which will also limit the maximum size of wires to the thickness of the membrane in use. Other processes, such as RABiTS,[6,7] CVD[8] and PLD[9,10] can be used to yield high performance 2D films; but very high time, substrate, reagent and equipment costs are generally prohibitive.

Biotemplating through sol–gel processing has enabled control over crystal morphology on a microscopic scale, with both high purity and/or anisotropic crystal growth in functional materials possible through use of dried polysaccharide gels[11,12] or solutions in ionic liquids.[13] High dimension/macroscopic architectures have also been demonstrated previously, inspired by the macroscopic morphology imposed by the template, such as diatom frustules,[14] pollen grains,[15] cuttlebone[16] or plant viruses.[17,18] Typically however, these templates are used for functionally benign materials such as silica; calcium phosphate and carbonate;[15] or polycrystalline copper[18] are crystallised hydrothermally, which is not generally possible for superconductors or other complex functional materials owing to the ease of formation of stable associate phases.

Higher order macroscopic structures of $YBa_2Cu_3O_{7-x}$ (Y123) have been previously reported employing cuttlebone, a porous, 3D calcitic structure, as a template.[19] Whilst Y123 can be generated as a decoration of the surface, it exists as a minority inorganic phase since the scaffold remains in a stable, oxidised form. In this work, a variety of 3D designed architectures of Y123 are demonstrated through sol–gel engineering with organic, starch/cellulose-blend templates (pasta). By employing a template composed predominantly of degradable organic materials, replication of the macroscopic structure through sacrificial templating is possible, with the desired inorganic phase remaining as the major phase. It is through ensuring Y123 is the predominant phase that the function as superconducting wires can be successfully demonstrated.

Precursors for superconducting Y123 replicas of pasta were formed from rehydration of prewashed pasta in aqueous solutions of yttrium, barium and copper nitrates. A moderate excess of $Ba(NO_3)_2$ was required to obtain higher proportions of the superconducting Y123 phase, due to a propensity for yielding mixed Ba-poor phases in stoichiometric precursors (CuO, Y_2O_3, and $Y_2Cu_2O_5$) and stable, high melting point $BaSO_4$ (effectively removing Ba^{2+} from molten eutectic at 920 °C) (Fig. S1 and S2, ESI†). Poor absorption of Ba^{2+} compared to Y^{3+} and Cu^{2+} due to lower solubility, larger ionic radius and favoured formation of $BaSO_4$ have been attributed to the requirement of an excess of barium. Prewashing assisted with the removal of impurities (see ESI†) which have a destructive effect on the properties of Y123; lowering T_c through crystal doping, preventing effective grain connectivity and reducing density. Specifically, the generation of $BaSO_4$ as confirmed by pXRD (Fig. S1a and b, ESI†) and TEM (Fig. S1c, ESI†) and the lower proportion of this phase generated with prewashed compared to unwashed precursors was observed (Fig. S1b, ESI†).

Y123-rich replicas of pasta shapes were generated through the calcination of pasta-based precursors (Fig. 1 and Fig. S2, ESI†). The macroscopic morphology of the pasta shape was retained leading to a range of different architectures, such as

[a] *Complex Functional Materials Group, School of Chemistry, University of Bristol, BS8 1TS, UK. E-mail: Simon.Hall@bristol.ac.uk*
[b] *Superconductivity and Magnetism Group, Physics Department, University of Warwick, Coventry, CV4 7AL, UK*

† Electronic supplementary information (ESI) available: Experimental details, Fig. (S1–S5) and Tables (S1 and S2). See DOI: 10.1039/c3cc38271k

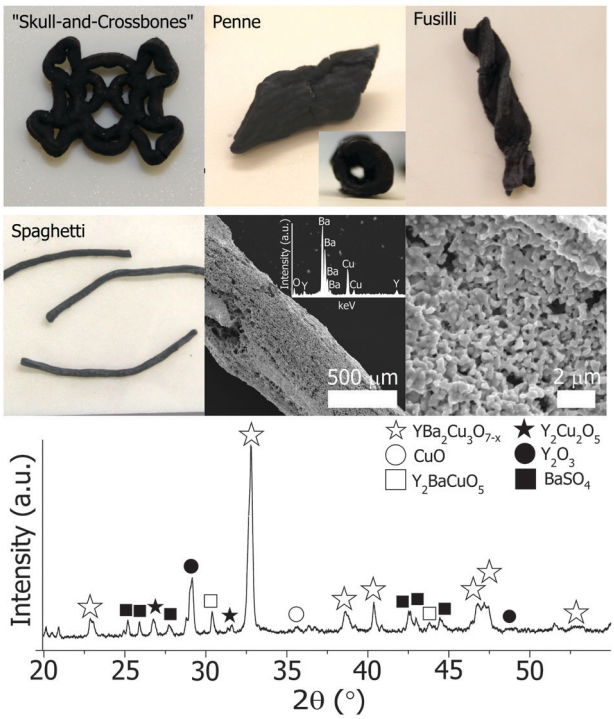

Fig. 1 Photographs of Y123-rich replicas of various pasta shapes as labelled. An inset is provided with 'penne' to demonstrate the retention of the tubular structure of the original pasta template. A typical pXRD pattern (bottom) demonstrates the predominance of Y123 in the replicas; however other phases have been labelled. SEM images of spaghetti replicas (bottom right) demonstrate the porous, low-density nature of the replicas and the expected elemental composition.

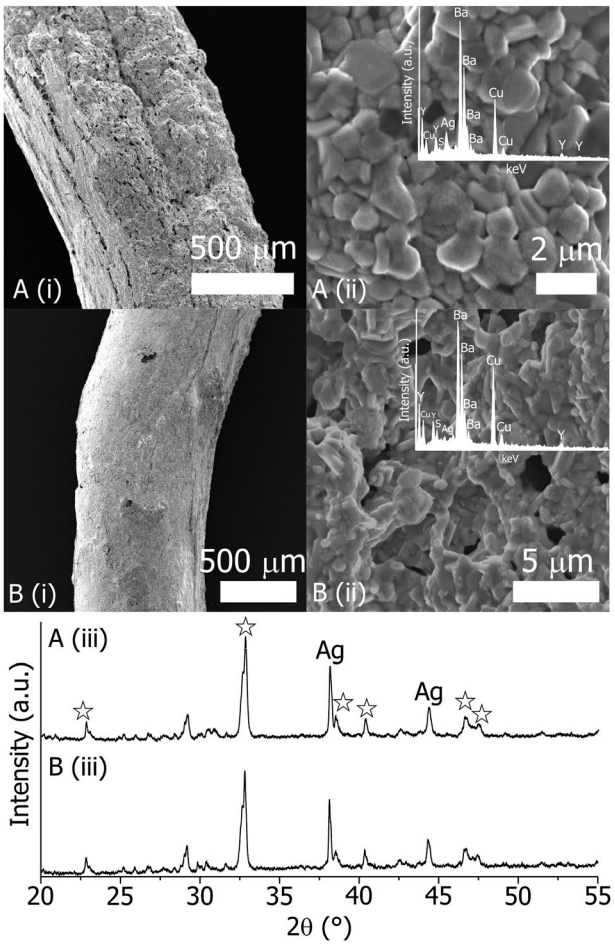

Fig. 2 SEM micrographs of Ag/Y123 replicas of spaghetti as calcined (A i and ii) and after sintering/annealing (B i and ii) with EDXA analysis demonstrating the presence of silver. Corresponding pXRD patterns (A iii and B iii) demonstrate little change in crystalline composition. Peaks indexed to Ag^0 ('Ag') and Y123 (star) are labelled.

wires, tubes or spirals from spaghetti, penne and fusilli respectively. The versatility of this protocol even allowed for the generation of more unusual morphologies such as a "skull-and-crossbones" motif. The overall Y123 content of these materials was 71% based on crystallographic analysis, taking the form of a highly porous, sponge-like microscopic structure formed from sintered crystallites (Fig. 1). This structure was expected from materials generated in the presence of high proportions of combustible, sacrificial templating agents: out-gassing of CO_2 at 400 °C as a result of combustion of starch and cellulose created pores as the gas escaped (Fig. S3a, ESI†). Despite the materials being self-supporting, they remained very weak and prone to destruction under minimal force due to the low density and low surface connectivity of the individual crystallites.

In order to improve conductive properties of Y123-rich spaghetti replicas, 10 wt% $AgNO_3$ was added to the precursor metal ion solution as rehydration of the spaghetti occurred. Silver has been shown to occupy intergranular sites between crystallites of Y123,[19,20] thereby increasing grain connectivity and mechanical strength, as well as metallic silver forming a conducting support to assist with electrical properties. In this case, the addition of silver to the synthesis doubled compressive strength from 0.76 to 1.56 MPa. Calcination products of Ag/Y123 precursors appeared similar to those of the Y123-only precursors; however a greater degree of shrinkage and densification occurred (Table S1, ESI†). Crystallographic analysis was also comparable except for the presence of Ag^0, formed from reduced Ag^+; thus the proportion of Y123 with respect to total crystalline content decreased to 60% (Fig. 2). The colour change observed on the generation of Ag/Y123 pasta precursor was attributed to starch-mediated reduction of Ag^+ to yield Ag nanoparticles.[21,22] Crystalline Ag^0 was detected before formation of precursory carbonates and oxides (Fig. S3, ESI†). While the product remained sponge-like, densification was evident due to the larger crystallite sizes, greater grain connectivity and decrease in overall pore size (Fig. 2 and Fig. S4, ESI†).

Due to the elongated, 1D nature of the replicas formed from spaghetti, their possible function as an electrically conducting wire was tested. Superconducting quantum interference device (SQUID) magnetometry demonstrated comparable T_c's for samples with and without the presence of Ag, with T_c = 70.25 and 72.05 K respectively (Fig. 3 and Fig. S5, ESI†). Critical current densities (J_c) at 1 T and 10 K calculated from the smallest dimension of measurable crystalline size were 0.157 and 0.478 MA cm^{-2} for Ag/Y123 and Y123 materials respectively (Fig. S5, ESI†). For both critical parameters, these are low when compared to typical values obtained for Y123 generated in other syntheses, with a diminished T_c of over 20 K and a J_c lowered between 2 and 3 orders of magnitude.

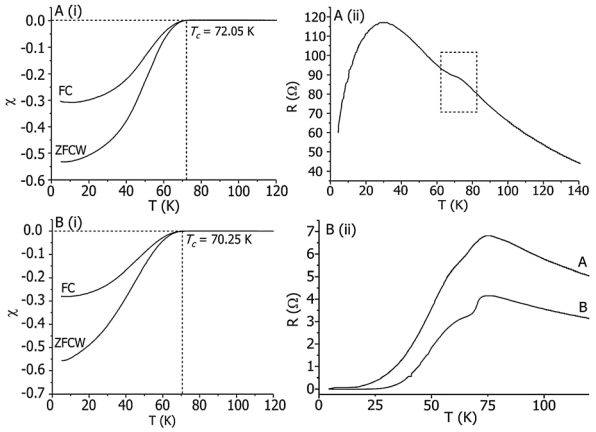

Fig. 3 *M vs. T* (i) and *R vs. T* (ii) plots for Y123-only (A) and Ag/YBCO. In (i), FC = field cooling, ZFCW = zero field cooled warming. Superconducting transition in Y123-only sample (A ii) indicated with a box. Differences can be observed in Ag/Y123 materials, where A = calcined product and B = post sinter and anneal.

Diminished T_c's were attributed to the presence of deleterious impurities doping the Y123 crystal, such as Zn^{2+}, Fe^{3+} and Ca^{2+} which are present in the pasta as purchased from food retailers (Table S2, ESI†).

Moderately higher J_c in Y123 compared to Ag/Y123 was attributed to greater porosity, which increases vortex pinning, however the overall depression observed in both samples was attributed to the altered crystalline phase present due to dopants.

Despite similarities in the T_c's, 4-point probe resistivity measurements demonstrated stark differences in conductive behaviour. In the Ag/Y123 materials, semicondutor-like behaviour was observed as the resistance increased with decreasing temperature until a sudden decrease in resistance was observed at a critical temperature (T_c = 74 K), where resistance continued to decrease from 6.82 Ω to 0.006 Ω at 4.2 K (Fig. 3). In the Y123-only material of equivalent length and shape, transition into the superconducting state was observed, however the resistance continues to increase until T = 29 K, when resistance began to decrease (Fig. 3). The overall resistance maximum of the Y123-only materials was much higher, with R = 116.8 Ω at 29 K. The superior performance of the Ag/Y123 materials was attributed to increased grain connectivity and intercrystalline surface contact as a result of higher density. Ag^0 acts therefore as a structural support and also provides an ohmic contact between the superconducting crystallites to facilitate electrical conductivity in the superconducting state.

An increased T_c and an immeasurably low resistance were attained through further sintering of the Ag/Y123 spaghetti replica (Fig. 3). 12 h sintering at 900 °C densified the replica, increasing average maximum crystallite size and grain connectivity; 8 h annealing at 500 °C ensured full oxygenation of the Y123 phase. T_c increased to a maximum of 78.52 K after both sintering and annealing, with $T_{R=0}$ = 22 K. No further increase in mechanical strength was observed beyond that of the pre-sintered material.

In summary, a range of 3D self-supporting architectures have been developed by employing pasta as a sacrificial template. Y123-rich replicas of spaghetti, penne and fusilli have been demonstrated, as well as more complex, unusual structures such as a skull-and-crossbones motif. Potential application of Ag/Y123 replicas of spaghetti, selected due to their elongated, 1D morphology, as superconducting wires has also been demonstrated, and, in spite of a depressed T_c and low J_c, immeasurably low resistance has been achieved at 22 K. High-purity templates and further densification are proposed measures to improve performance. This report demonstrates the application of a simple, widely-available, cost-effective, sacrificial template in the synthesis of a complex functional material, and may be developed further to inspire and create novel architectures for functional materials suited for a desired purpose.

This research was funded by a University of Bristol DTA. Professor Antony Carrington, Mr Carsten Putzke, Dr Liam Malone and Mr Phil Walmsley of the School of Physics, University of Bristol, UK are gratefully acknowledged for their assistance with the resistance measurements. The magnetometer used in this research was obtained through the Science City Advanced Materials project: Creating and Characterizing Next Generation Advanced Materials project, with support from Advantage West Midlands (AWM) and part funded by the European Regional Development Fund (ERDF).

Notes and References

1 R. W. Schwartz, *Chem. Mater.*, 1997, **9**, 2325.
2 P. Vermeir, I. Cardinael, M. Bäcker, J. Schaubroeck, E. Schacht, S. Hoste and I. Van Driessche, *Supercond. Sci. Technol.*, 2009, **22**, 075009.
3 B. A. Albiss and I. M. Obaidat, *J. Mater. Chem.*, 2010, **20**, 1836.
4 I. Van Driessche, J. Feys and S. C. Hopkins, *et al.*, *Supercond. Sci. Technol.*, 2012, **25**, 065017.
5 J. Xu, X. Liu and Y. Li, *Mater. Chem. Phys.*, 2004, **86**, 409.
6 A. Goyal, D. P. Norton and D. K. Christen, *et al.*, *Appl. Supercond.*, 1996, **4**, 403.
7 M. W. Rupich, U. Schoop and D. T. Verebelyi, *et al.*, *IEEE Trans. Appl. Supercond.*, 2003, **13**, 2458.
8 N. Dechoux, C. Jiménez and P. Chaudouë, *et al.*, *Supercond. Sci. Technol.*, 2012, **25**, 125008.
9 D. Marré, A. Diaspro, C. Ferdeghini, G. Grassano, I. Pallecchi and A. S. Siri, *Supercond. Sci. Technol.*, 1998, **11**, 737.
10 Y. Yu, X. Zhang, J. W. Wang and Y. G. Zhao, *J. Cryst. Growth*, 2012, **354**, 98.
11 S. R. Hall, *Adv. Mater.*, 2006, **18**, 487.
12 Z. A. C. Schnepp, S. C. Wimbush, S. Mann and S. R. Hall, *Adv. Mater.*, 2008, **20**, 1782.
13 D. C. Green, S. Glatzel, A. M. Collins, A. J. Patil and S. R. Hall, *Adv. Mater.*, 2012, **24**, 5767.
14 Z. Bao, M. R. Weatherspoon, S. Shian, Y. Cai, P. D. Graham, S. M. Allan, G. Ahmad, M. B. Dickerson, B. C. Church, Z. Kang, H. W. Abernathy III, C. J. Summers, M. Liu and K. H. Sandhage, *Nature*, 2007, **446**, 172.
15 S. R. Hall, H. Bolger and S. Mann, *Chem. Commun.*, 2003, 2784.
16 W. Ogasawara, W. Shenton, S. A. Davis and S. Mann, *Chem. Mater.*, 2000, **12**, 2835.
17 M. Young, D. Willits, M. Uchida and T. Douglas, *Annu. Rev. Phytopathol.*, 2008, **46**, 361.
18 J. C. Zhou, C. M. Soto, M.-S. Chen, M. A. Bruckman and M. H. Moore, *et al.*, *J. Nanobiotechnol.*, 2012, **10**, 18.
19 E. Culverwell, S. C. Wimbush and S. R. Hall, *Chem. Commun.*, 2008, 1055.
20 D. Walsh, S. C. Wimbush and S. R. Hall, *Chem. Mater.*, 2007, **19**, 647.
21 V. Ernest, P. J. Shiny, A. Mukherjee and N. Chandrasekaran, *Carbohydr. Res.*, 2012, **352**, 60.
22 Z. Shervani and Y. Yamamoto, *Carbohydr. Res.*, 2011, **346**, 651.

